Carbohydrate Research, 160 (1987) 73–93
Elsevier Science Publishers B V , Amsterdam – Printed in The Netherlands

CARBON-13 MAGNETIC RELAXATION AND LOCAL CHAIN MOTION OF AMYLOSE IN DIMETHYL SULFOXIDE

PHOTIS DAIS
Department of Chemistry, McGill University, Montreal, Quebec H3C 3G1 (Canada)
(Received May 8th, 1986, accepted for publication in revised form, August 2nd, 1986)

ABSTRACT

The nature of internal and overall modes of reorientation in amylose dissolved in dimethyl sulfoxide at 80° is examined by a variety of dynamic models using multifield relaxation parameters T_1, T_2, and n.O.e. The overall motion appears to be that of an axially symmetric cylinder, with rotational correlation times in good agreement with those calculated from hydrodynamic theory, assuming helical segments comprising 40–50 monomer residues. The internal motion can best be described as restricted-amplitude internal-diffusion of individual C–H vectors, with conic boundary conditions. A bistable jump model is a less favorable alternative, as it requires a physically unrealistic angle between the C-1, H-1 vector and the jump axis. The critical role of chain conformation and chain stiffness on dynamic modelling is discussed, as well, on the basis of earlier studies.

INTRODUCTION

Interest in the motional behavior of polysaccharides in solution has grown in recent years. In particular, measurements of ^{13}C spin–lattice relaxation times (T_1) have been carried out in several instances[1–6] for linear polysaccharides, in order to probe variations in segmental motion of terminal groups, and for branched polysaccharides, to investigate differences in mobility between side-chain residues and those incorporated in the backbone. Experiments such as these have facilitated the assignment of ^{13}C-resonance signals that were difficult to identify on the basis of chemical shifts, and have provided a qualitative description of mobility as reflected in T_1 values. Although qualitative analysis of ^{13}C relaxation data appears to be useful in describing gross features of the mobility of carbohydrate chains, it is less valuable than quantitative information inherent in the measurement of spin–lattice relaxation times.

A complete interpretation of relaxation data requires a suitable, dynamic model that reflects the geometric constraints that characterize a molecule and its possible modes of reorientation. Several dynamic models[7–13] have been developed in recent years to describe the dynamics of synthetic polymers in solution. However, their applicability to the relaxation of polysaccharides[14,15] appears to be

0008-6215/87/$ 03 50

limited, as shown[15] clearly for the case of amylose in dimethyl sulfoxide. The ineffectiveness of these models for describing the dynamics of carbohydrate molecules may be explained on the basis of the specific nature of a carbohydrate chain as compared with a hydrocarbon chain. A carbohydrate chain typically contains a large number of monosaccharide units bound together through glycosidic linkages. These monomer units oscillate about the glycosidic bonds with an amplitude that is determined mainly by geometric constraints. Theoretical calculations[16–19] in the form of conformational-energy maps have shown that the majority ($\geq$90–95%) of linkage orientations for disaccharides, and particularly for polysaccharides, are forbidden, mainly by nonbonded interactions. Conformational constraints of this severity do not comply with the tetrahedral, diamond-lattice arrangement of a carbohydrate chain, which is a major working-hypothesis for the lattice-dynamic models[10–12]. Moreover, the inherent implication, in these models, that local motions involving a few monomer units within the chain should be accompanied by relatively large conformational changes along the main chain, cannot be accommodated by the relatively stiff amylose chain. It appears that local motions, described as crankshaft conformational jumps[10–12], or other types of cooperative motions[7–9,13], cannot optimally interpret the relaxation data of carbohydrate chains.

It has been suggested[15] that local conformational changes in carbohydrate chains can be expressed as oscillatory, or other, types of motion within a disaccharide unit. These motions, the amplitude of which depends on geometric constraints within the simple kinetic unit, introduce an angular dependence of the C–H, dipole–dipole interactions, a fact that may explain the observed[15] differences in the T_1 values of C-1 and the remaining ring carbon atoms in amylose. In this report, the aforementioned remarks are critically examined, for amylose in $(CD_3)_2SO$ at 80°, through dynamic modeling, supplemented by measurements of ^{13}C spin–spin relaxation times (T_2) and of viscosity.

EXPERIMENTAL

The multifield, ^{13}C T_1 and n.O.e values for each carbon nucleus of amylose obtained previously[15] will be used in the present study. These data, together with additional measurements for the carbon nucleus conducted on a Varian XL-300 spectometer at 75.4 MHz, are summarized in Table I. Experimental details for measuring ^{13}C T_1 and n.O.e. values are reported elsewhere[15].

Measurements of ^{13}C spin–spin relaxation times at four frequencies were performed by the Carr–Purcell–Meiboom–Gill method[20], with complete noise decoupling of protons. However, to avoid an irreversible diminution in the measured ^{13}C T_2 values as compared to the true values[21], the noise decoupling was switched off during echo formation, but reestablished during acquisition and over a long delay time ($\sim 2 \times T_1$) before initiation of the pulse sequence The 180° pulse was carefully determined with a 90% w/v solution of methyl α-D-glucoside in

TABLE I

FIELD DEPENDENCE OF THE ^{13}C SPIN-LATTICE AND SPIN-SPIN RELAXATION TIMES (ms) AND n O e VALUES FOR THE VARIOUS CARBON NUCLEI OF AMYLOSE IN $(CD_3)_2SO$ SOLUTION AT 80°

Carbon atom	*Beta (degrees)*		*100 MHz*			*75 MHz*			*50 MHz*			*20 MHz*		
			T_1	T_2	*n O e*	T_1	T_2	*n O e*	T_1	T_2	*n O.e*	T_1	T_2	*n O e.*
C-1	82 0[a],	37 0[b]	224 ±10	105 ±5	1 58 ±0 04	182 ±4	91 ±3	1 70 ±0 02	127 ±9	75 ±5	1 90 ±0 13	79 ±6	58 ±5	2 24 ±0 08
C-2	99.0,	75 6	255 ±12	119 ±6	1 63 ±0 07	197 ±4	107 ±2	1 69 ±0.07	150 ±9	84 ±2	1 86 ±0 09	86 ±7	65 ±3	2 20 ±0.06
C-3	72 3	75 0	253 ±15	119 ±2	1 68 ±0 11	203 ±5	105 ±2	1 72 ±0 06	154 ±11	87 ±2	2 02 ±0 16	90 ±10	65 ±4	2 10 ±0.07
C-4	75.3	67 0	251 ±9	115 ±4	1 59 ±0 07	194 ±5	108 ±3	1 71 ±0 08	144 ±13	87 ±3	1 83 ±0 03	88 ±9	64 ±6	2 08 ±0 06
C-5	79 9	57 3	249 ±8	117 ±5	1 65 ±0.11	204 ±7	108 ±5	1 75 ±0 04	151 ±10	89 ±5	1 89 ±0 06	88 ±8	61 ±3	2 12 ±0 09
C-6	—	—	152 ±10	82 ±6	1 64 ±0 08	130 ±9	68 ±5	1 81 ±0 05	90 ±8	54 ±3	2 02 ±0.09	62 ±6	38 ±6	2 25 ±0 09

[a]These values represent the angle β between the C–H vector and the z-axis [b]Angles formed between the C–H vector and the virtual bond

$(CD_3)_2SO$. The duration of the 180° pulse train covered a range of about 0.01 to 3 times the largest T_1 value. The measured T_2 values are summarized in Table I, along with the standard deviation of the mean value of at least two measurements.

Viscosity measurements were carried out by using a modified Ubbelohde type of viscometer in a bath thermostatted at 80° ±0.01. The $(CD_3)_2SO$ solvent was first dried by refluxing over CaO for 24 h, followed by distillation under diminished pressure. The intrinsic viscosity was determined by plotting η_{sp}/C *vs.* C, and extrapolating to zero concentration. This value was found to be 104.7 mL/g. The Huggins constant, derived from the slope of the same plot, was $k' = 0.414$, in good agreement with the literature value[22] (0.431).

The weight-average molecular weight ($\overline{M}_w$) was determined by sedimentation–diffusion equilibrium analysis to be 3.3×10^5. The dependence of $\overline{M}_w$ on the rotor speed indicated that the amylose sample was a polydisperse polymer.

RESULTS AND DISCUSSION

The general approach used to extract the maximum amount of information from the relaxation data of a complex molecular system, such as amylose, involves the following consideration: (*1*) an *a priori* knowledge of the nature of the system under investigation. This may assist in critically assessing the various modes of reorientation that contribute to the relaxation of the molecule; (*2*) the formulation of a reasonable model that describes the overall and internal motions of the system; (*3*) the possibility that the relaxation data may be described by several models; and (*4*) whether or not the experimental data and the nature of the system can eliminate one or other model and, for a given model, whether a unique parameter set can reproduce the experimental data.

Conformation of the amylose chain, and modes of reorientation. — The geometric constraints in the amylose chain arise primarily from nonbonded interactions between the α-(1→4)-linked D-glucosyl monomer residues in the minimum-energy, $^4C_1$ conformation[23–25]. These constraints, which are expressed in terms of torsional angles ϕ and ψ, introduce severe restrictions upon the domain of the conformational space accessible to the backbone units. Additional constraints must be imposed on the conformational freedom of the D-glucosidic bond, especially in solvents of poor solvating power, by intramolecular hydrogen-bonding between OH-2 of one α-D-glucosyl residue and OH-3 of the adjacent residue[24,25]. Theoretical calculations predict[17,18,26,27] that the area of such a conformational space is only ~1.5% for amylose. Nevertheless, even though the majority of linkage conformations are forbidden, the remaining conformational space allows for significant freedom of oscillation about the D-glucosidic bridge. These oscillatory motions within a disaccharide unit constitute the local internal motions of amylose. Motions extended to include a few monomer units along the chain seem improbable, as discussed earlier[15], or, if they exist, they probably occur through small, continuous changes of the dihedral angles of D-glucosidic bonds along the allowed low-energy

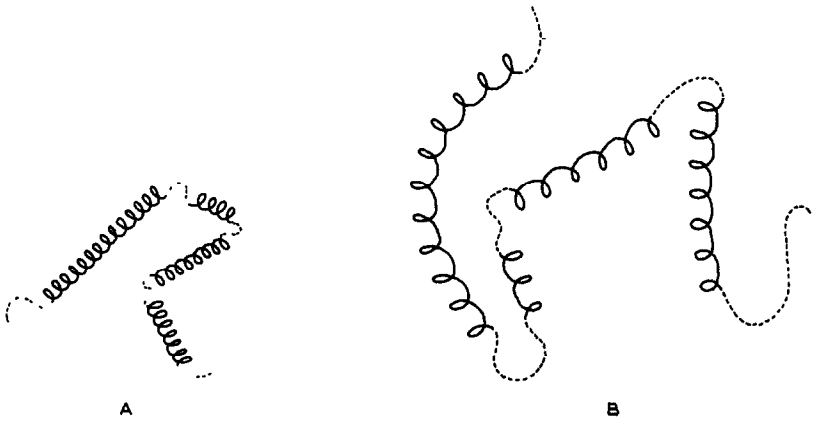

Fig. 1 Schematic representation of two different models for the conformation of amylose in aqueous solution. [(A) The tight helix model, and (B) the extended-helix model The dotted segments designate disordered regions]

surface within the conformational space. Motions of this type, associated with distortions of valence lengths and angles from their equilibrium values, are not considered in the present treatment. Bond lengths and angle distortions are characterized by much larger force-contants than those for torsional strain involving rotations about the D-glucosidic bonds, with the consequence that motions of the former type are of relatively small thermal amplitude[28,29] and, hence, have a negligible effect on dipolar relaxation.

The magnitude of the internal fluctuations about the D-glucosidic bond determines the chain configuration. The greater the internal freedom at each linkage, the greater the number of conformations available to each individual residue, and, hence, the less likely is the chain to adopt a unique, ordered, shape in which each linkage is in a minimum-energy form. Chain flexibility thus provides a strong entropic drive, which generally overcomes energy factors, and induces disordered or "random coil" states in solution[30]. By contrast, such favorable energy terms as hydrogen bonding, solvent effects, and severe nonbonded interactions can combine to fix the macromolecule into ordered shapes. These cooperative interactions occur along extended sequences in the chain, and result in a helical or pseudohelical conformation. Despite extensive investigation, which of these competing factors dominates in solution, to shape the amylose chain, is still a matter of controversy. Most interpretations of the various theoretical[26,27,31] and experimental[30,32–36] data support the proposition that, in neutral aqueous solution, amylose behaves as a "random coil" with short, loosely wound, helical segments as depicted schematically in Fig. 1. In $(CD_3)_2SO$ solution, the persistence of intramolecular hydrogen-bonding in the disaccharide unit may help to stiffen the chain, due to an increase in the helical content and the compactness of the helical segment[24,25,36–38]. Although, for aqueous amylose, the helical segment may contain

more than 100 monomer units[36,39] in $(CD_3)_2SO$, this number, as well as the average number of helical sections in a single chain, are unknown parameters.

To complete the assessment of the various modes of reorientation in amylose, collective motions should be considered as well. The first collective motion is an end-over-end rotation of the persistence vector or, in other words, the orientation of the macromolecule as a whole. This motion depends on the overall molecular shape, which is, in turn, determined by the magnitude of the internal motions around the D-glucosidic bond, *i.e.*, chain stiffness, or chain flexibility, or both. Other collective motions, such as a reorientation of helical segments in the chain, involving several monomer units, cannot be excluded in describing collective motions, on a faster scale than the overall mode of reorientation.

Dynamic models for the amylose chain. — A description of the local and overall modes of reorientation in terms of a dynamic model must take into consideration to the local geometric constraints and conformation of amylose in solution. The local constraints can take the form either of boundary conditions of restricted amplitude of internal diffusion (diffusion models), or potential barriers associated with discrete jumps among equivalent or non-equivalent, stable conformations (jump models). Which of these models better describes the dynamics of amylose will be determined by how well it reproduces relaxation data in physically realistic terms.

The mathematical formulation of the model and its constraints is used to obtain an autocorrelation function[40,41], $C(t)$, which describes how the motion contributes to n.m.r. spin relaxation. The spectral density function[40,41], $J(\omega)$, which describes the efficiency of n.m.r. spin relaxation in terms of motional frequency components is obtained, by Fourier transformation of the autocorrelation function, as

$$J(\omega) = \int_{-\infty}^{+\infty} C(t)\, e^{i\omega t}\, \mathrm{d}t. \qquad (1)$$

For a single correlation time, τ_c, the spectral density function takes the form[41]

$$J(\omega) = \frac{\tau_c}{1 + \omega^2\tau_c^2}. \qquad (2)$$

Analytical expressions relating the spectral density function to observable relaxation parameters arising from dipole–dipole interactions are given by[41]

$$\frac{1}{T_1} = \frac{1}{10}\frac{\gamma_H^2\gamma_C^2\hbar^2}{r_{C\text{-}H}^6}\,[J(\omega_H - \omega_C) + 3J(\omega_C) + 6J(\omega_H + \omega_C)], \qquad (3)$$

$$\frac{1}{T_2} = \frac{1}{20}\frac{\gamma_H^2\gamma_C^2\hbar^2}{r_{C-H}^6}[4J(0) + J(\omega_H - \omega_C) + 3J(\omega_C) + 6J(\omega_H) + 6J(\omega_H + \omega_C)], \quad (4)$$

$$\text{and n.O.e.} = 1 + \frac{\gamma_H}{\gamma_C}\frac{J(\omega_H - \omega_C) + 6J(\omega_H + \omega_C)}{J(\omega_H - \omega_C) + 3J(\omega_C) + 6J(\omega_H + \omega_C)}. \quad (5)$$

In Eqs. *3–5*, γ_H and γ_C are the gyromagnetic ratios of the proton and carbon nuclei, respectively, ω_H and ω_C are their respective Larmor frequencies, and r_{C-H} is the C–H bond length.

An important assumption inherent in the formulation of the autocorrelation function of a model is that internal and overall motions of the molecule are mutually independent, and thus uncorrelated. In this case, the total correlation function can be rigorously factored out as[42]

$$C(t) = C_O(t) \cdot C_I(t), \quad (6)$$

where $C_O(t)$ and $C_I(t)$ are the autocorrelation functions for overall and internal motions, respectively.

For isotropic, overall motion of the amylose chain, the corresponding autocorrelation function is a slowly decaying function (correlation time $\sim 10^{-6}$ s), whereas the autocorrelation function for internal motion decays faster (correlation time 10^{-9}–10^{-10} s), and hence, Eq. *6* represents a good approximation for the total autocorrelation function. When the overall motion is anisotropic, the total autocorrelation function cannot be factored rigorously into a product of contribution due to overall and internal motions, even when it is assumed that these motions are independent. Nevertheless, Eq. *6* will be retained as a first approximation to the problem. The validity of this decoupling approximation will be apparent later in this study, while modeling the dynamics of amylose.

Overall molecular motion. — Due to uncertainty as to the conformation of the amylose molecule chain, its overall motion will be characterized by rotational correlation-times for either isotropic or anisotropic rotational diffusion. The former model corresponds to an almost spherical shape of a "random coil", whereas the latter model is compatible with the reorientation of helical-chain segments consisting of several monomer units. The nature of the overall motion will be established according to which model fits the data. Rotational correlation times can be determined from relaxation data for carbon nuclei, which relax mainly *via* the overall molecular motion. However, because this does not apply for amylose, the parameters of its overall motion must be simulated from other experiments, *e.g.*, hydrodynamic, or light-scattering, measurements.

Overall isotropic motion is described by a single correlation time, τ_R', which is given at infinite dilution by[43]

$$\tau_R' = \frac{2\,\overline{M}_w\,[\eta]\,\eta_0}{3\,R\,T}, \tag{7}$$

η_0 is the solvent viscosity. In a solution of finite concentration, C, the correlation time, τ_R, is estimated from the following equation[44]

$$\ln(\tau_R/\tau_R') = k'\,[\eta]\,C, \tag{8}$$

where k' is the Huggins constant. The effect of the molecular weight distribution can be taken into account by incorporating into Eq. *8* a Schultz–Zimm[45] molecular-weight-distribution function, $W(x)$, given by[45]

$$W(x) = \frac{\eta^{k+1}\,\bar{x}_w^k\,e^{-\eta\bar{x}_w}}{\Gamma(k+1)}, \lambda = \frac{k+1}{\bar{x}_w} \tag{9}$$

The breadth parameter k in Eq. *9* depends on the breadth of the distribution, $\bar{x}_n/\bar{x}_w$, where $\bar{x}$ is the number average degree of polymerization. No experimental estimate of polydispersity can be made, because only the $\overline{M}_w$ was measured. However, studies of a large number of amylose samples show[22,38,46–50] that the breadth of the distribution lies between 1.3 and 2.0. Therefore, a distribution of $\bar{x}_n:\bar{x}_w = 1:5$ is a reasonable estimate for the amylose sample measured here. If this distribution is used, then $k = 2$ in[45] Eq. *9*, and, from Eqs. *7–9*, we obtain $\tau_R = 7.0 \times 10^{-6}$ s. It should be noted that varying the choice of the distribution between 1.3 and 2.0 does not result in an uncertainty greatly different from that inherent in the simulation of the τ_R value.

The possibility for anisotropic motion of helical-chain segments that may behave hydrodynamically like cylinders can be described by two correlation times: $\tau_\parallel$, which describes rotational diffusion about the major axis of the cylinder, and is given by the relation[51]

$$\tau_\parallel = \frac{\pi\,\eta_0\,L^3}{18kT}[\ln(L/b) - 1.57 + 7[1/\ln(L/b) - 0.28]^2]^{-1}, \tag{10}$$

and the correlation time, $\tau_\perp$, of the short axis of the cylinder, given by[52]

$$\tau_\perp = \frac{8\pi\eta_0\,b^2L}{6\,k\,T}, \tag{11}$$

where $L = 1.355\,n$ (Å), the axial length of the cylinder, which depends on the number n of monomer units in the helical segment, and b is the transverse radius of the cylinder. The coefficient 1.355 Å corresponds to the pitch per D-glucosyl residue in the helix of the amylose–$(CD_3)_2SO$ complex, as obtained from crystallographic data[53]. The structure of this complex was selected because it represents a

TABLE II

ROTATIONAL CORRELATION TIMES CALCULATED FROM EQS *10* AND *11* AS A FUNCTION OF THE MONOMERIC D-GLUCOSYL RESIDUES PER HELICAL SEGMENT

Monomer residues	L *(Å)*	τ $(10^{-8}$ s)	$\tau_{\parallel}(10^{-9}$ s)
20	27 10	0 08	0.52
30	40 65	0.27	0 79
40	54.20	0.54	1.05
50	67 75	0 90	1.31
60	81 30	1 37	1.57
70	94 85	1 96	1.84
80	108 40	2 69	2 10
90	121 95	3 56	2 36
100	135 50	4 60	2 62
120	162 60	7.21	3 15
150	203 25	12.60	3 93
170	230 04	17 26	4 45
200	271.00	26 24	5 25

useful conformational pattern for amylose in solution in terms of helical conformation and hydrogen bonding by the $(CH_3)_2SO$ molecules. The crystal structure of amylose–$(CH_3)_2SO$ is depicted in the *xy* projection in Fig. 3 of ref. 53, which also defines the helical axis used in subsequent treatment of internal motion. Radius *b* is obtained from the relationship $b = (2/3)^{1/2}\sigma$, where $\sigma = 6.15$ Å is the hydrodynamic radius of an individual monomer[35]. Table II summarizes the correlation times calculated from Eqs. *10* and *11* as a function of the number of monomer units per helical segment.

A simple correlation time does not fit the data in Table I. This is evident from a simple calculation using Eqs. *2–5* for dipolar relaxation. The same is true in treating amylose as a rigid rod whose rotational behavior is described by two correlation times, $\tau_{\perp}$, using the Woessner formalism[54(a)] for motional anisotropy of an axially symmetric molecule. Therefore, some kind of internal motion may have to be considered in order to interpret the relaxation data in Table I.

Internal motion. — There are several models that treat internal motion: free or restricted rotation about a bond[54–56], a wobbling motion in which the relaxation vector diffuse within a cone[57–61], or various jump models[55,62–64]. The internal motion is superimposed on either an isotropic or an anisotropic overall motion. All of the models take into account the different β angles for the C–H vectors and an axis that may be the *z*-axis of an ellipsoid or the internal jump axis (or rotation), thereby introducing an angular dependence of the dipolar relaxation of the various carbon sites. This angular dependence is incorporated in the autocorrelation function or in its Fourier transform, the spectral density function.

Internal motion superimposed on an isotropic, overall motion will be considered first. I begin with the internal, 2-state jump-model of London[62(c)], which

describes internal jumps between two stable states A and B, with lifetimes τ_A and τ_B. The relevant spectral density is given by[62(c)]

$$J(\omega) = (1 - C)\frac{\tau_R}{1 + \omega^2\tau_R^2} + C\frac{\tau_N}{1 + \omega^2\tau_N^2}, \tag{12}$$

where

$$\tau_N^{-1} = \tau_R^{-1} + \tau_C^{-1} \text{ and } \tau_C^{-1} = \tau_A^{-1} + \tau_B^{-1} \tag{13}$$

$$\text{and } C = \frac{3\tau_A\tau_B}{(\tau_A + \tau_B)^2}[\sin^2\beta\ (1 - \cos 2\theta)]\ [2 - \sin^2\beta\ (1 - \cos 2\theta)]. \tag{14}$$

Here, the angle β is defined by the C–H vector and the axis about which the vector jumps, and θ is one-half the jump range (*i.e.*, jumps in between $-\theta$ and $+\theta$).

Restricted-amplitude internal-diffusion constitutes another important general class of motion[56b]. Restricted diffusion about a single axis has been solved analytically[56b], and the resulting spectral density is

$$J(\omega) = \sum_{i=-2}^{+2}\sum_{n=0}^{\infty} |\mathbf{E}(i,n)|^2|\mathbf{d}_{io}(\beta)|^2\frac{\tau_n}{1 + \omega^2\tau_n^2}, \tag{15}$$

where

$$\tau_n^{-1} = \tau_R^{-1} + \frac{n^2\pi^2}{24\,\tau_i\theta^2} \tag{16}$$

Here, β is the angle between the relaxation vector and the internal axis of rotation, 2θ defines the allowed range of motion, τ_i is the correlation time which describes internal motion, $\mathbf{d}_{io}(\beta)$ is the reduced Wigner rotation matrix[65], whereas the matrix $\mathbf{E}(i,n)$ is given in ref. 56b.

Internal librational motion of a C–H vector superimposed on an isotropic overall motion has been treated by Howarth[59] in an attempt to explain the existing experimental anomalies concerning the relaxation behavior of large peptides and proteins. According to this model, a C–H vector is free to take up any direction within a cone defined by a fixed orientation θ, and its random jumps between different directions are assumed to be governed by the single correlation time τ_G. The spectral density $J(\omega)$ arising from such a motion originally, derived by Woessner[54(a)], can be found in ref. 59.

Internal motion superimposed on an anisotropic overall motion of helical segments within the amylose chain will be considered next. The simplest possibility

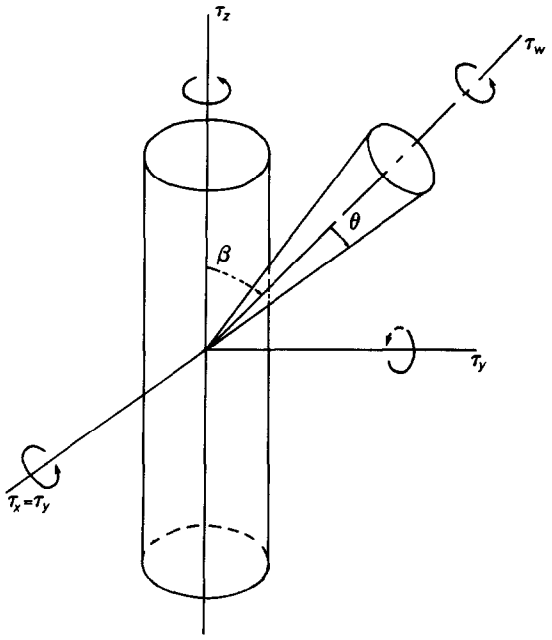

Fig. 2 Diffusion in a cone model

is a wobble or spaghetti-like motion of the backbone, with approximately conical boundary conditions. This motion is superimposed on overall tumbling that is axially symmetric. Being a flexing motion of limited amplitude, it promotes internal motion of the individual C–H vectors, which are also assumed to be restricted by similar, conical-boundary conditions. The motional problem of a conical boundary condition has been examined by several authors[57–61], the most complete and convenient treatment of these being due to Lipari and Szabo[61(b,c)]. In this model, depicted schematically in Fig. 2, internal motion is described as a wobbling in a cone, so that the C–H vector moves freely at a given rate, τ_w, inside the conical boundary defined by an angle θ, but has zero probability of being found outside the boundary. β is the angle that the director of the cone makes with the z-axis, and τ_z and $\tau_x = \tau_y$ are the correlation times for rotation about the z- and x (or y)-axes of the cylinder. Lipari and Szabo[61(b)] obtained an analytical expression for the auto-correlation function, $C(t)$, of this model

$$C(t) = \sum_{k,m=-2}^{+2} \exp\{-[6D_x + k^2(D_z - D_x)t]\} \, |\mathbf{d}_{km}(\beta)|^2 C_I(t) \tag{17}$$

$$\text{and } C_I(t) = C_m(\infty) + [C_m(0) - C_m(\infty)] \exp[-t/\tau_i^{(m)}] \tag{18}$$

$$\text{where } \tau_i^{(m)} = [C_m(0) - C_m(\infty)]^{-1} \tau_m. \tag{19}$$

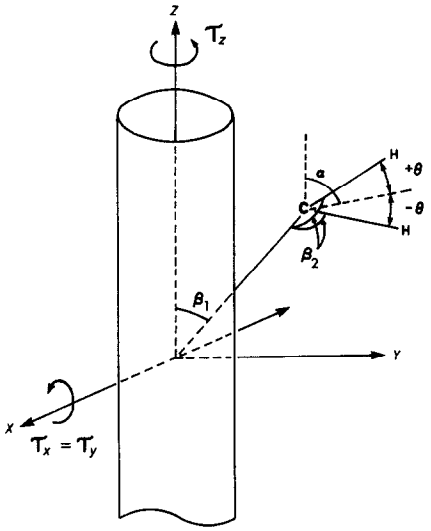

Fig 3 Bistable jump model

Simple closed-form expressions of $C_m(0)$, $C_m(\infty)$ and $\tau_l^{(m)}$ in terms of θ and τ_w are given in ref. 61(c). The parameter $D_x = D_y$ and D_z are diffusion coefficients for overall motion of the cylinder, and are related to correlation times by

$$D_j = \frac{1}{6\tau_j}, j = x, y, \text{ and } z. \tag{20}$$

In addition to internal motion restricted within a conical boundary, there are a number of other types of restricted motion that have been used to model motion in complex biological systems[55,56,62–64,66]. Some of these models have been discussed previously.

I proceed with a bistable model developed by London and Phillipi[62(a)], in which the relaxation vector jumps internally between two stable states, A and B, with lifetimes τ_A and τ_B, respectively. The extent of the jump or jump range is defined by angle 2θ (*i.e.*, the jump is between $-\theta$ and $+\theta$, with respect to the bisector, as in Fig. 3). Also, the internal jump motion is superimposed on anisotropic overall motion described by the τ_z and $\tau_x = \tau_y$ rotational correlation times; β_1 describes the angle between the z-axis and the internal jump axis; β_2 describes the angle between the jump axis and the C–H vectors. The orientation of the bisector relative to the z-axis is described by angle α, the physical significance of which has been discussed elsewhere[62(a)]. The resulting autocorrelation function has the form

$$C(t) = \sum_{a,b,b'=-2}^{+2} A_{aa'} \mathbf{d}_{ab}(\beta_1) \cdot \mathbf{d}_{ab'}(\beta_1) \cdot [(\mathbf{A}'^{(1)}_{bb'} + \mathbf{A}'^{(2)}_{bb'}) \cos(b - b')\alpha$$

$$- \mathbf{A}'^{(3)}_{bb'} \sin(b - b')\alpha] \cdot \mathbf{d}_{bo}(\beta_2) \cdot \mathbf{d}_{b'o}(\beta_2), \tag{21}$$

where, $\mathbf{d}_{ab}(\beta)$ are, as before, the reduced Wigner rotation matrices

$$A_{aa'} = \exp\{-[6D_x + a^2(D_z - D_x)]t\} \cdot \delta_{aa'}, \tag{22}$$

and the matrices $\mathbf{A}'^{(1)}$, $\mathbf{A}'^{(2)}$, and $\mathbf{A}'^{(3)}$ are

$$\mathbf{A}'^{(1)}_{m,m'} = (1 - k)\cos(m - m')\theta + k\cos(m + m')\theta, \tag{23}$$

$$\mathbf{A}'^{(2)}_{m,m'} = k[\cos(m - m')\theta - \cos(m + m')\theta]\, e^{-t/\tau_c}, \tag{24}$$

and $$\mathbf{A}'^{(3)}_{m,m'} = \mathrm{i}\, k' \sin(m - m')\theta. \tag{25}$$

Also,

$$k = \frac{2\tau_A\tau_B}{(\tau_A + \tau_B)^2}, k' = \frac{(\tau_A^2 - \tau_B^2)}{(\tau_A + \tau_B)^2}, \tag{26}$$

and τ_C are given by Eq. *13*.

Recently, Lipari and Szabo[67] considered a model-free approach to the interpretation of n.m.r. relaxation data for macromolecules in solution. Both isotropic and anisotropic overall motions combined with various models for internal motion were considered. The data were analyzed in terms of two model-independent parameters, the generalized order parameter, S, which is a measure of the degree of spatial restriction of the motion, and the effective correlation time, τ_e, which is a measure of the rate of the motion. These parameters are extracted either by least-squares fitting to the experimental data, or, in favorable cases, by using simple analytical forms, and are compared with exact values generated from a variety of motional models describing internal motion. Models without sufficient flexibility to reproduce the numerical values of S *and* τ_e extracted from the experiment are eliminated. Such a model-free formalism can be very useful in characterizing the molecular dynamics of such highly flexible, chain molecules as random-coil polymers. However, for such molecules as amylose, having a stiff, helix-like chain, even though a model-free approach may describe the data, it does not optimally interpret the data in physically realistic terms.

Numerical calculations. — The first step to be taken in order to analyze the relaxation data of amylose within the context of a dynamical model is to examine the geometry of the molecule, from which axes of rotation and the various fixed

angles can be defined. Relating the various models to the helix-like structure of amylose, I assume that the reference is the helical chain segment subject to the overall motion defined by the helix axis, as in the solid state[53]. This implies that all monomer residues within a helical segment have the same z-axis, which is aligned with the helix axis. Considering restricted rotation or jumps about an internal axis, I assume that the reference segment is the α-D-glucosyl residue defined by a rotation (or jumps) axis, which coincides with the virtual bond, *i.e.*, the vector spanning the D-glucopyranosyl residue and joined at the bridge-oxygen atom as shown in Fig. 4. The concept of virtual bond or pseudobond has been successfully introduced into several theoretical treatments[26(a,c),27,29] of the conformation of amylose, and represents a reasonable approximation in the present analysis.

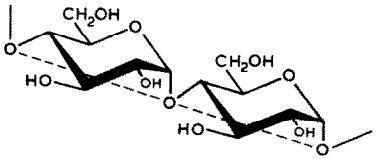

Fig. 4. Schematic representation of a disaccharide residue of amylose, showing the definition of the virtual bond (broken line).

Values were determined (see Table I) for the C–H bond angles with respect to the z-axis (the helix axis of amylose) and internal axis (the virtual bond), based on atomic coordinates obtained for amylose[53,68,69]. The angle formed between the virtual bond and the z-axis was found to be 71.5°. As the values of β for the C–H vector of C-2 and of C-5 differ, it is unlikely that rapid torsional motion about the z-axis can account for the similar relaxation data observed for these carbon atoms, as noted previously in treating amylose as a rigid rod. Rapid torsional motion of limited amplitude, superimposed on an isotropic overall motion can, in principle, offer an alternative explanation for short T_1 values and significant n.O.e.; nevertheless, this approach would predict for the various carbon atoms relaxation parameters that are not functions of angle β formed by the z-axis and the C–H vector.

Several of the models were tested by using the powerful MOLDYN program[70] implemented by Levy and co-workers[71]. Among other functions[71], the program can be used to optimize parameter values for a given model, to provide the best fit to a set of experimental data. Any number of parameters may be optimized for a given model, provided that a sufficiency of experimental data is available. Also, initial guesses and convergence criteria should be specified before proceeding with the calculation. The optimization procedure is based on the SIMPLEX algorithm[71] minimizing the normalized sum of squares of deviations between calculated and observed relaxation data (T_1, T_2, and n.O.e.). The sum of squares of deviations can be used as a measure of goodness of fit. This statistical parameter depends on the number of adjustable parameters, the precision and the

TABLE III

COMPARISON OF N M R PARAMETERS FOR C-2 ACCORDING TO VARIOUS MODELS FOR AMYLOSE[a] AND THOSE OBSERVED EXPERIMENTALLY

Model	*Magnetic field (MHz for carbon)*	T_1	T_2	*n O e*
Isotropic motion	20	80	≤0 01	2 10
+ internal 2-state jump[b]	50	149	≤0 01	2.01
	75	200	≤0.01	1 66
	100	252	≤0.01	1 48
Isotropic motion	20	84	≤0 01	2.46
+ internal amplitude	50	144	≤0 01	1 86
restricted diffusion[c]	75	195	≤0.01	1 67
	100	253	≤0 01	1 57
Isotropic motion	20	66	7	2.67
+ internal libration	50	108	7	2 30
(Howarth)[d]	75	140	7	1 94
	100	173	7	1 70
Axially symmetric motion	20	78	67	2 24
+ internal rotation[e]	50	133	90	2.20
	75	176	103	2.11
	100	218	112	2 00
Observed	20	86	65	2.20
	50	150	84	1.86
	75	197	107	1.69
	100	255	119	1 63

[a]Input parameters $\beta = 99°$ with respect to z-axis and 75.6° with respect to virtual bond; $\tau_R = 7.0 \times 10^{-6}$ s. The internal axis of rotation or the jump axis for these models coincides with the virtual bond [b]$\theta = 59\ 3°$, $\tau_A = \tau_B = 1\ 9 \times 10^{-9}$ s [ref 62(c)] [c]$\theta = 71.7°$, $\tau_i = 4\ 2 \times 10^{-10}$ s [ref 56(b)] [d]$\tau_G = 6\ 8 \times 10^{-9}$ s (ref 59) [e]$\tau_x = \tau_z = 5.5 \times 10^{-9}$ s, $\tau_{int} = 2\ 3 \times 10^{-10}$ s [ref 54(d)]

number of experimental data, the ability of the model chosen to describe the range and the type of motions present in the molecule, the convergency criteria, and the number of iterations for optimization. Values for this parameter of the order 10^{-2}–10^{-3} reflect a good fit.

The data for the C-2 atom are presented in Table III for the internal 2-state jump model[62(c)], internal amplitude restricted diffusion model[56(b)], and Howarth's internal libration model[59]. The fitting parameter for the various models and the input parameters β and τ_R are summarized as footnotes in Table III. It is evident that none of the models reproduce the T_2 data, nor do such physical parameters as angles θ have realistic values. Also, the Howarth model does not reproduce the T_1 and n.O.e. data (see Table III).

I proceed with the axially symmetric + internal conic diffusion model[61(b,c)]. The calculated relaxation data in Table IV are in very good agreement with the

TABLE IV

^{13}C RELAXATION DATA CALCULATED[a] FOR AMYLOSE AXIALLY SYMMETRIC + INTERNAL CONIC DIFFUSION[b]

Carbon atom	*Beta (degrees)*	*100 MHz*			*75 MHz*			*50 MHz*			*20 MHz*		
		T_1	T_2	*n.O e*	T_1	T_2	*n O e*	T_1	T_2	*n.O e*	T_1	T_2	*n O.e*
C-1	82	243	102	1 57	188	93	1 69	132	80	1 90	68	56	2 20
C-2	99	264	115	1.66	206	106	1 75	147	91	1 92	77	64	2.22
C-3	72.3	258	124	1 63	199	112	1 70	141	95	1.86	76	65	2.23
C-4	75 3	260	121	1.64	202	110	1 72	145	93	1.91	77	65	2.20
C-5	79 9	264	117	1.66	206	107	1.75	147	92	1 93	78	65	2.18

[a]Fitting parameters: $\theta_{cone} = 31\ 8°$ for C-2 to C-5, and 26 1° for C-1, $\tau_x = 6\ 8 \times 10^{-9}$ s, $\tau_z = 6\ 0 \times 10^{-10}$ s, and $\tau_w = 1\ 4 \times 10^{-10}$ s [b]See text and refs 61(b) and 61(c) for this model

TABLE V

^{13}C RELAXATION DATA CALCULATED[a] FOR AMYLOSE AXIALLY SYMMETRIC + INTERNAL 2-STATE JUMP[b]

Carbon atom	*Beta (degrees)*	*100 MHz*			*75 MHz*			*50 MHz*			*20 MHz*		
		T_1	T_2	*n O e*	T_1	T_2	*n.O e*	T_1	T_2	*n O e*	T_1	T_2	*n O e*
C-1[c]	37 0	232	100	1 63	177	91	1 70	126	79	1 85	74	57	2 24
C-2	75 6	265	115	1 65	203	105	1 73	146	92	1 83	79	64	2 22
C-3	75 0	264	114	1 70	203	105	1 73	145	91	1 82	79	63	2 21
C-4	67 0	258	105	1 66	196	97	1 69	140	84	1.79	74	59	2 19
C-5	57 3	242	102	1 60	182	93	1 64	128	81	1 75	68	55	2 19

[a]Input parameters. $\beta_1 = 71.5°$, β_2 as in Table. Fitting parameters: $\alpha = 48\ 9°$, $\theta = 25\ 1°$, $\tau_A = \tau_B = 1\ 6 \times 10^{-10}$ s, $\tau_x = 1\ 3 \times 10^{-8}$ s, $\tau_z = 4\ 0 \times 10^{-10}$ s [b]See text and ref 62(a) for this model [c]$\beta_2 = 48\ 9°$ and $\alpha = 17\ 5°$

experimental values, and the fitting parameters, θ_{cone}, τ_w, $\tau_x = \tau_y$, and τ_z are reasonable. In particular, the $\tau_x = \tau_y$ and τ_z correlation times, compared with the $\tau_\perp$ and $\tau_\parallel$ correlation times in Table II, are commensure with a helical chain segment consisting, on the average, of 40–50 monomer residues. Good agreement between the calculated and experimental data is observed (see Table V) as well, using the bistable model of London and Phillips[62(a)]. The fitting parameters are the angles a and θ, and the correlation times, $\tau_A = \tau_B$, $\tau_x = \tau_y$ and τ_z. The $\tau_x = \tau_y$ and τ_z values for this model are consistent with a helical segment comprising, on the average, 20–60 monomer residues.

From Tables I, IV, and V, it is clear that both the wobbling-in-a-cone and bistable-jump models are able to reproduce the experimental data. However, the wobbling-in-a-cone model is mainly favored, for two reasons. First, it requires fewer adjustable parameters than the bistable-jump model in order to fit the data, and second, the fitting by the jump model requires $\beta_2 = 48.9°$ for the C-1 atom, which is physically unrealistic.

For purposes of comparison, I have considered axially symmetric motion plus internal rotation[54(d)]. This model does not reproduce the experimental data (see Table III), as expected, because free rotation is unlikely to occur in this highly strained molecular system.

Relaxation of the C-6 (exocyclic) atom. — The relaxation data for C-6 in Table I suggest that the methylene C–H vectors undergo relatively faster motion about the C-5–C-6 bond of the D-glucopyranose ring. This stems from the fact that the T_1 value of C-6 (moderated by two protons) is longer than the T_1 values of the ring-carbon atoms. However, intramolecular hydrogen-bonding either between[68] OH-6 and OH-2, or between two adjacent OH-6 groups and $(CD_3)_2SO$ molecules[53], restricts the amplitude of rotation. It is worth mentioning in this respect that, for a fast-rotating group with tetrahedral angles, T_1 will be 9 times longer than in the absence of internal motion[72]. A bistable jump model[62–64], or an internal amplitude-restricted diffusion model[56(b)], or both, may be suitable in describing the relaxation data as a function of the parameter θ, which defines the amplitude of motion. In this way, C-6 internal motion can be described by an extended model, in which the total correlation function contains contributions from: (*1*) overall motion represented by the diffusion of an axially symmetric cylinder, (*2*) restricted amplitude diffusion-in-a-cone, and (*3*) a bistable jump or restricted diffusional motion for C-6, all of which have already been discussed.

CONCLUSION

The present study attempted to describe the nature of internal motion and overall reorientation of amylose in $(CD_3)_2SO$ solution, and how these are reflected in the measured multifield relaxation parameters. The motion-in-a-cone model appears to be the most reasonable basis for analysis at present, and may represent an approximately realistic description of internal motion. Also, the relaxation data

lead to several interesting conclusions about the nature of the overall molecular diffusion. Isotropic-motion models either do not fit the data, or require unrealistic assumptions about the parameter values. All such models must clearly be rejected in favor of a much more ordered dynamic process, with relatively short helical segments within the amylose chain comprising 40–50 monomer residues. Details about the motion of the exocyclic hydroxymethyl group are less clear. However, C-6 appears to be affected by an additional restricted-amplitude motion.

ACKNOWLEDGMENTS

The author is grateful to Prof. A. S. Perlin for valuable discussions and continuous encouragement. Generous support by McGill University and the Natural Sciences and Engineering Research Council of Canada is gratefully acknowledged. The 100- and 20-MHz T_2 measurements were performed at the Laboratoire Regional de RNM à Haut Champ, Université de Montréal.

REFERENCES

1 P A. J. Gorin, *Adv. Carbohydr. Chem. Biochem.*, 38 (1981) 13–104.
2 A. S. Perlin and B. Casu, in G. O. Aspinall (Ed.), *The Polysaccharides*, Vol. 1, Academic Press, New York, 1982, Chapter 4.
3 F R. Seymour and R. D. Knapp, *Carbohydr. Res.*, 81 (1980) 67–103.
4 K Dill and A. Allerhand, *J. Biol. Chem.*, 254 (1979) 4524.
5 M. Vignon, F. Michon, and J.-P Joceleau, *Macromolecules*, 16 (1983) 835–838.
6 A. J. Benesi and D A. Brant, *Macromolecules*, 18 (1985) 1109–1116.
7 F. Heatley and M. K. Cox, *Polymer*, 18 (1977) 225–232.
8 D. Ghesquiere, B. Ban, and C. Chachaty, *Macromolecules*, 10 (1977) 743–752.
9 J Schaefer, *Macromolecules*, 6 (1973) 882–888.
10 A. A. Jones and W. H. Stockmayer, *J. Polym Sci., Polym. Phys Ed*, 15 (1977) 847–861.
11 (a) B. Valeur, J. P Jarry, F. Geny, and L. Monnerie, *J. Polym Sci., Polym. Phys. Ed.*, 13 (1975) 667–674; (b) B. Valeur, L. Monnerie, and J. P. Jarry, *ibid*, 13 (1975) 675–682; (c) B. Valeur, J. P. Jarry, F Geny, and L. Monnerie, *ibid.*, 13 (1975) 2251
12 J Bendler and R. Yaris, *Macromolecules*, 11 (1978) 650–655.
13 (a) C. K. Hall and E. Helfand, *J Chem. Phys.*, 77 (1982) 3275–3282; (b) T. A. Weber and E. Helfand, *J. Phys Chem.*, 87 (1983) 2881–2889.
14 K. Matsuo, *Macromolecules*, 17 (1984) 449–452.
15 P. Dais, *Macromolecules*, 18 (1985) 1351–1354.
16 V. S. R. Rao, P R Sundararajan, G Ramakrishnan, and G. N. Ramachandran, in G N. Ramachandran (Ed.), *Conformation of Biopolymers*, Academic Press, New York, 1967
17 D. A. Brant, *Q. Rev. Biophys.*, 9 (1976) 527–596.
18 D. A. Brant and B. A. Burton, *Solution Properties of Polysaccharides, ACS Symp. Ser.*, 150, (1980).
19 D. A. Rees, E. R. Morris, D. Thom, and J. K. Madden, in G. O. Aspinall (Ed.), *The Polysaccharides*, Vol 1, Academic Press, New York, 1982, Chapter 5.
20 S Meiboom and D. Gill, *Rev. Sci. Instrum.*, 29 (1958) 688–691.
21 R. R. Ernst, *J. Chem. Phys.*, 45 (1966) 3845–3861.
22 W W. Everett and J. F Foster, *J. Am. Chem. Soc.*, 81 (1959) 3464–3469
23 V. S. R. Rao and J. F Foster, *J. Phys. Chem.*, 69 (1965) 636–640.
24 B. Casu and M. Reggiani, *Tetrahedron*, 22 (1966) 3061–2083.
25 M. St -Jacques, P R. Sundararajan, J. K. Taylor, and R. H. Marchessault, *J. Am Chem. Soc.*, 98 (1976) 4386–4391.

26 (a) D A BRANT AND W. L DIMPFL, *Macromolecules*, 3 (1970) 655–664, (b) K. D. GOEBEL, W L DIMPFL, AND D A BRANT, *ibid.*, 3 (1970) 644–654; (c) R C JORDAN, D A BRANT, AND A CESARO, *Biopolymers*, 17 (1978) 2617–2632
27 S. G. WHITTINGTON AND R M GLOVER, *Macromolecules*, 5 (1972) 55–58
28 D A BRANT, *Annu. Rev. Biophys Bioeng*, 1 (1972) 369–408
29 D A BRANT AND K D GOEBEL, *Macromolecules*, 8 (1975) 522–530
30 D. A REES, *Polysaccharide Shapes*, Chapman & Hall, London, 1977
31 V S R RAO, N YATHINDRA, AND P R SUNDARARAJAN, *Biopolymers*, 8 (1969) 325–333
32 D. A REES, *M.T.P Int Rev Sci, Biochem., Ser One*, 5 (1975) 1–49.
33 M KODAMA, H NODA, AND T KAMATA, *Biopolymers*, 17 (1978) 985–1002
34 D G LEWIS AND W C JOHNSON, *Biopolymers*, 17 (1978) 1439–1449
35 (a) H ELMGREN, *Biopolymers*, 23 (1984) 2525–2541, (b) B EBERT AND H ELMGREN, *ibid.*, 23 (1984) 2543–2557
36 R L WHISTLER AND J R DANIEL, in R L WHISTLER, J N BEMILLER, AND E F PASCHALL, (Eds), *Starch Chemistry and Technology*, 2nd edn , Academic Press, New York, 1984, Chapter VI
37 F R DINTZIS AND R TOBIN, *Biopolymers*, 7 (1969) 581–593
38 M FUJII, K HONDA, AND H. FUJITA, *Biopolymers*, 12 (1973) 1177–1195
39 W BANKS AND C. T. GREENWOOD, *Starch and its Components*, University Press, Edinburgh, 1975
40 A A ABRAGAM, *The Principles of Nuclear Magnetism*, Oxford Univ Press, London, 1961, Chapter 8
41 J R LYERLA AND G. C LEVY, in G C. LEVY (Ed), *Topics in Carbon-13 NMR Spectroscopy*, Vol 1, Wiley–Interscience, New York, 1974, Chapter 3
42 D WALLACH, *J. Chem. Phys*, 47 (1967) 5258–5268
43 A. ISIHARA, *Adv Polym. Sci*, 5 (1968) 531–567.
44 R P LUBIANEZ, A. A. JONES, AND M BISCEGLIA, *Macromolecules*, 12 (1979) 1141–1145
45 G. V. Z SCHULTZ, *Z Phys Chem, Abt B*, 43 (1939) 25–46; (b) B H ZIMM, *J Chem. Phys*, 16 (1948) 1099–1116
46 S G. RING, K J L'ANSON, AND V J MORRIS, *Macromolecules*, 18 (1985) 182–188
47 W BURCHARD, *Makromol Chem*, 59 (1963) 16–27.
48 J M. C COWIE, *Makromol. Chem*, 42 (1961) 230–247
49 W W EVERETT AND J F FOSTER, *J Am Chem. Soc*, 81 (1959) 3459–3464
50 K D GOEBEL AND D A BRANT, *Macromolecules*, 3 (1970) 634–643
51 S BROERSMA, *J Chem. Phys*, 32 (1960) 1626–1631
52 H LAMB, *Hydrodynamics*, Dover, New York, 1945
53 W T WINTER AND A SARKO, *Biopolymers*, 13 (1974) 1461–1482
54 (a) D. E WOESNER, *J Chem Phys*, 36 (1962) 1–4; (b) 37 (1962) 647–654; (c) 42 (1965) 1855–1859; (d) D E WOESSNER, B S SNOWDEN, JR , AND G H. MEYER, *ibid.*, 50 (1969) 719–721
55 R J WITTEBORT AND A. SZABO, *J Chem Phys*, 69 (1978) 1722–1736
56 (a) R E LONDON AND A AVITABILE, *J Chem Phys*, 65 (1976) 2443–2450; (b) *J Am Chem Soc*, 100 (1978) 7159–7165
57 C C WANG AND R PECORA, *J Chem Phys*, 72 (1980) 5333–5340
58 R RICHARZ, K NAGAYAMA, AND K WUTHRICH, *Biochemistry*, 19 (1980) 5189–5196
59 O W. HOWARTH, *J Chem Soc, Faraday Trans 2*, 75 (1980) 1031–1041
60 T E BULL, *J Magn Reson.*, 31 (19789 453–458
61 (a) G LIPARI AND A SZABO, *Biophys J*, 30 (1980) 489–506; (b) *Biochemistry*, 20 (1981) 6250–6256, (c) *J Chem Phys*, 75 (1981) 2971–2976, (d) J R BRAINARD AND A SZABO, *Biochemistry*, 20 (1981) 4618–4628
62 (a) R E LONDON AND M A PHILLIPI, *J Magn Reson*, 45 (1981) 476–489, (b) R E LONDON AND A AVITABILE, *J Am Chem Soc*, 99 (1977) 7765–7776; (c) R E LONDON, *ibid*, 100 (1978) 2678–2685
63 A TSUTSUMI, *Mol Phys*, 39 (1979) 111–127
64 (a) R. KING AND O JARDETZKY, *Chem Phys Lett*, 55 (1978) 15–18, (b) R KING, R MAAS, M GASSNER, R K NANDA, W W CONOVER, AND O JARDETZKY, *Biophys J*, 24 (1978) 103–117; (c) A A RIBEIRO, R KING, C RESTIVO, AND O JARDETZKY, *J Am Chem Soc*, 102 (1980) 4040–4051
65 M E ROSE, *Elementary Theory of Angular Momentum*, Wiley, New York, 1957, Chapter 4
66 G C LEVY, D J CRAIK, A KUMAR, AND R E LONDON, *Biopolymers*, 22 (1983) 2703–2726

67 (a) G. LIPARI AND A. SZABO, *J. Am. Chem. Soc.*, 104 (1982) 4546–4559; (b) 4559–4570
68 W T WINTER AND T. SARKO, *Biopolymers*, 13 (1974) 1447–1460
69 S. ARNOTT AND W. E. SCOTT, *J Chem. Soc., Perkin Trans. 2*, (1972) 324–335.
70 D. J. CRAIK, A KUMAR, AND G. C. LEVY, *MOLDYN*, Quantum Chemistry Program Exchange, 1983, No 489
71 D. J CRAIK, A. KUMAR, AND G. C. LEVY, *J. Chem Inf. Comput Sci*, 23 (1983) 30–38
72 A ALLERHAND, D DODDRELL, AND R KOMOROSKI, *J Phys. Chem.*, 55 (1971) 189–198.